Front. Earth Sci. 2016, 10(4): 644–661
DOI 10.1007/s11707-015-0548-x

RESEARCH ARTICLE

An assessment of precipitation and surface air temperature over China by regional climate models

Xueyuan WANG, Jianping TANG (✉), Xiaorui NIU, Shuyu WANG

1 School of Atmospheric Sciences, Nanjing University, Nanjing 210093, China
2 Institute for Climate and Global Change Research, Nanjing University, Nanjing 210093, China

Abstract An analysis of a 20-year summer time simulation of present-day climate (1989−2008) over China using four regional climate models coupled with different land surface models is carried out. The climatic means, interannual variability, linear trends, and extremes are examined, with focus on precipitation and near surface air temperature. The models are able to reproduce the basic features of the observed summer mean precipitation and temperature over China and the regional detail due to topographic forcing. Overall, the model performance is better for temperature than that of precipitation. The models reasonably grasp the major anomalies and standard deviations over China and the five subregions studied. The models generally reproduce the spatial pattern of high interannual variability over wet regions, and low variability over the dry regions. The models also capture well the variable temperature gradient increase to the north by latitude. Both the observed and simulated linear trend of precipitation shows a drying tendency over the Yangtze River Basin and wetting over South China. The models capture well the relatively small temperature trends in large areas of China. The models reasonably simulate the characteristics of extreme precipitation indices of heavy rain days and heavy precipitation fraction. Most of the models also performed well in capturing both the sign and magnitude of the daily maximum and minimum temperatures over China.

Keywords regional climate model, interannual variation, trend, extremes

1 Introduction

Along with the development of global climate observational systems and the rapid expansion of high performance computer techniques, interest in climate numerical modeling has been steadily increasing since the 1980s. Regional climate models (RCMs) have been increasingly used to produce climate change information at the regional scale due to higher resolution and better representation of key physical processes than global climate models (GCMs) (e.g., Liang et al., 2004a, b, 2012; Liu et al., 2013). Since the RCMs can accurately describe regional details in surface climate characteristics such as topography and land-use distribution, the RCMs have shown promise in better capturing smaller climate system information and variation than GCMs. As a result, a number of RCMs have been developed and recognized as efficient and necessary tools for studying regional climate (Feng and Fu, 2006; Giorgi et al., 2012). RCMs were originally developed and applied in the simulation of regional climate by Dickinson et al. (1989) and Giorgi (1990). Since then, significant attention has been focused on RCMs development and has been applied in regional climate modeling more frequently.

China is located at East Asia and is greatly influenced by the typical monsoon climate. The particular geographic environment, complexity of vegetation distribution, and significant land use and cover changes due to intensive human activities makes the East Asian monsoon the most vigorous and influential of all the monsoon circulations (Zhao, 2013). Therefore, this region has very large climate variability on seasonal, interannual, decadal, and even centurial timescales (Feng and Fu, 2006). In recent years, people and governments are paying more attention to climate change. As both society and the economy continue to develop, future policy dictates a greater need for further study of regional climate modeling. These climate changes make it necessary for the development of RCMs that correctly model the East Asian Monsoon System. However, accurate prediction of China's climate is challenging due to complex surface characteristics and multiscale physical processes.

Received April 29, 2015; accepted July 1, 2015

E-mail: jptang@nju.edu.cn

Systematic studies are needed to quantify uncertainties in regional climate changes, to identify the sources of those uncertainties, and ultimately to reduce them.

In China, regional climate modeling began in the 1990s. At that time, the research was focused on case studies and sensitivity experiments (Fu et al., 1998; Tang et al., 2003). In recent years, the long term climate simulations over China and East Asia using different RCMs have been widely documented. These experiments provided valuable information on mean climate states simulation (Feng and Fu, 2006; Gao et al., 2011; Hu and Wang, 2011; Zhao, 2013), future climate change projection (Hu et al., 2012; Liu et al., 2013), and extreme climate events prediction (Feng et al., 2011; Hu et al., 2013). The Regional Climate Model Inter-comparison Project (RMIP) for Asia was started in 2000 (Fu et al., 2005) to identify model errors in simulating the East Asian climate. Phase I and II results have shown that most of the RCMs can basically reproduce the spatial distribution and the annual variation of the temperature and precipitation over East Asia (Fu et al., 2005; Feng and Fu, 2006, 2007).

To better understand the regional climate change over China, an analysis of the present-day climate simulations conducted by four RCMs is conducted and compared with observations through the 1989−2008 summer months . The main objects in this study are to evaluate the model performance for precipitation and temperature, and to analyze the regional climate change signal over China as affected by the different modeling systems and land use models. The analysis presented here, including climatic means, interannual variability, linear trends, and extremes, mostly focuses on precipitation and near surface air temperature over China as a whole and five subregions. In addition, the 850 hPa air circulation is presented in order better assess the model behavior. Section 2 describes the model and experiment designs, and the simulation results are discussed in Section 3. The summary and discussion are given in Section 4.

2 Description of models, simulations, and observations

2.1 Model description

We analyzed present climate simulations performed by four RCMs coupled with land surface models. The models include: 1) RegCM4-CLM, a new version of the RegCM regional climate modeling system, which added the option to use the Community Land Model, version CLM3.5 (Giorgi et al., 2012); 2) WRF-CLM, The Weather Research and Forecasting model version 3 coupled with CLM3.5 (Subin et al., 2011); 3) WRF-NOAH, The Weather Research and Forecasting model version 3 coupled with NOAH, which is one of the default options of the land surface model in WRF; and 4) RSM-NOAH, the National Centers for Environmental Prediction (NCEP) Regional Spectral Model (RSM) coupled with NOAH.

The RegCM model is a community-based, compressible, hydrostatic, and primitive-equation model originally developed by Giorgi et al. (1993a, b) and then augmented and discussed by Giorgi and Mearns (1999) and Pal et al. (2007). The WRF model is a fully compressible and non-hydrostatic model with terrain following pressure coordinate and Arakawa C-grid, which has been widely used for regional climate modeling (Katragkou et al., 2015). The NCEP RSM (Juang et al., 1997; Yhang and Hong, 2008) model is a primitive equation model using the sigma-vertical coordinate, and has been extensively applied to dynamic downscaling and operational short-range forecasting. The spectral representation of the RSM is a two dimensional cosine and sine series, and it is applied to the difference between the full field and the time-involving background global analysis field. The CLM3.5 land surface model (Oleson et al., 2008) is a state-of-the-art land surface scheme representing land surface processes in the context of climate simulations. The land component of the Community Climate System Model (CCSM) (Collins et al., 2006) and earlier versions of CLM3.5 have also been coupled to other regional climate models (Steiner et al., 2009; Tawfik and Steiner, 2011). The Noah Land Surface Model (LSM) has a long history of development through multi-institutional cooperation and has been widely used by the National Centers for Environmental Prediction (NCEP) in operational weather and climate predictions. The development efforts have improved the model performance in both offline (Chen et al., 2007) and coupled modes (Ek et al., 2003).

Table 1 shows the physical process and land surface parameterization for the four models. The differences between the models are attributed to model dynamics and land surface process.

2.2 Experiment design

Figure 1 illustrates the model computational domain. It covers the whole of China with horizontal grid cells of 223×167 in the east-west and north-south directions. The models use a 30 km horizontal grid spacing by the Lambert conformal map projection centered at (35°N, 108.5°E). The models include 28 vertical layers with the top at 50 hPa. The buffer zones are located across 12 grids along each of four domain edges. Outlined also in Fig. 1 are five subregions (Northeast China, North China, Yangtze River Basin, South China, and Northwest China) over which detailed result analysis are presented. These regions have been identified with distinct climate regimes and precipitation characteristics in both the annual cycle and interannual variability (Liu et al., 2013; Hu et al., 2013).

The simulation period is from 15th March to 1st October in each year, and the models run year by year from 1989 to 2008. The first 15 days in each year simulation is model

Table 1 The physical parameterizations of the models

	RegCM4-CLM	WRF-CLM	WRF-NOAH	RSM-NOAH
Convection	MIT-Emanuel	Kain-Fritsch scheme	Kain-Fritsch scheme	RAS
Microphysics	SUBEX	WSM 3-class simple ice scheme	WSM 3-class simple ice scheme	CLD3
Longwave radiation	CAM	CAM scheme	CAM scheme	Chou
Shortwave radiation	CAM	CAM scheme	CAM scheme	Chou
Planetary boundary layer	Holtslag	YSU scheme	YSU scheme	MRF
Land surface	CLM3.5	CLM3	NOAH	NOAH
Soil thermal layers	10	10	4	4

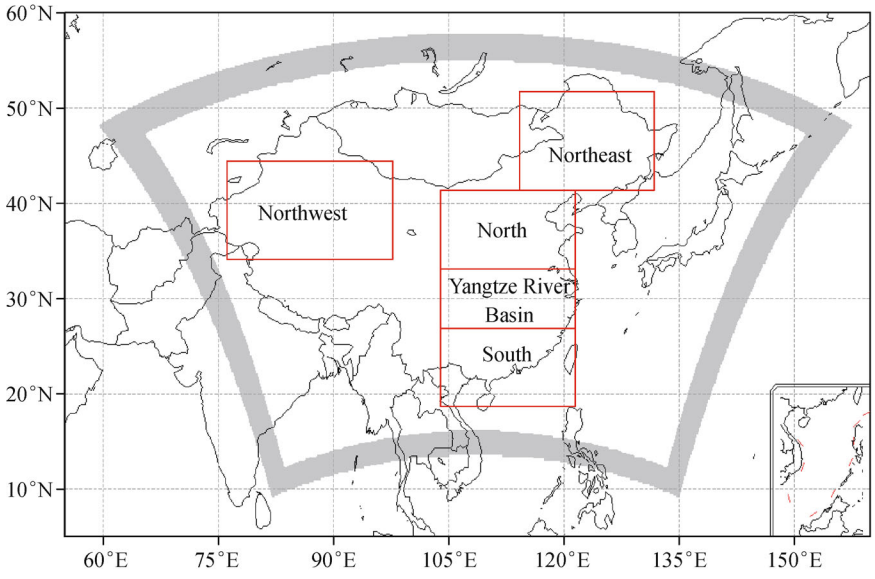

Fig. 1 The computational domain. Outlined are five analysis regions as labeled; the shaded edge areas are the buffer zones where lateral boundary conditions are specified.

spin-up, from which the output is not used for analysis. Our analysis is focused on summer time (including the three months of June, July, and August) precipitation and temperature averaged during the 20-year period.

The four models use the same initial and boundary conditions, which are constructed from the National Centers for Environmental Prediction/Department of Energy (NCEP/DOE) Reanalysis 2 (R2) data (Kanamitsu et al., 2002), available every 6 hours at 2.5°×2.5° grid spacing resolution (http://rda.ucar.edu/datasets/ds091.0/). The R2 data include air temperature, pressure, humidity, sea level pressure, winds, and geopotential height. The geographical data and meteorological fields on 15th March of each year are interpolated for the initial conditions. The meteorological fields are interpolated every 6 hours horizontally and vertically for the model buffer zones as boundary conditions. The models use the same surface vegetation and land use types by the United States Geological Survey from satellite information. The same driving field, simulation domain, and horizontal resolution ensure that the model differences only come from the model dynamics, physical parameterizations, and land surface models. The details of the model physical information are given in Table 1.

2.3 Observations

The daily gridded precipitation dataset (Yatagai et al., 2009) used for validation in this study was developed by the Research Institute for Humanity and Nature (RIHN) and the Meteorological Research Institute/Japan Meteorological Agency (MRI/JMA). The data was created by collecting rain gauge observational data across Asia through the activities of the Asian Precipitation Highly Resolved Observational Data Integration Towards the Evaluation of Water Resources (APHRODITE) project. The up to date APHRO_v1101R2 data, released in March 2013, is the only long-term (1961–2007) continental-scale daily product that contains a dense network of daily rain gauge data for Asia. The data is available at http://www.chikyu.ac.jp/precip/, and has a regular 0.25° resolution. Since the APHRO_v1101R2 data exists only up to 2007,

the model comparison for precipitation uses the first 19-year summer time period of 1989–2007, and the simulation of 2008 is only used for temperature evaluation.

The temperature data for model validation is the gridded daily temperature dataset of the National Climate Center of China Meteorological Administration (CN05). The dataset is based on the interpolation from 751 observing stations in China and comprises daily mean, minimum, and maximum temperature (Xu et al., 2009). The data set covers the period of 1961–2009 over mainland China and is gridded to a common latitude/longitude grid of 0.5°×0.5°. The CN05 dataset shows general agreement with CRU (Climatic Research Unit) data at the monthly scale (Xu et al., 2009). Hong et al. (2014) compared five gridded datasets including CN05 and found that country-wide trends in temperature extremes are coherent among the datasets. The CN05 dataset has been widely used in regional climate model evaluation (Yu et al., 2010; Chen et al., 2011; Gao et al., 2011; Guo et al., 2013; Dong et al., 2015).

In the comparison of observations and simulations, the simulations are interpolated onto 0.25°×0.25° resolution for precipitation and 0.5°×0.5° resolution for temperature, which fit the APHRO and CN05 (hereafter refers to observation for simplicity) data respectively. All the measurements are calculated at individual grid points and then, when needed, are averaged over the subregions of Fig. 1. Only land points are considered in the analysis.

3 Results

3.1 Seasonal means and biases

Figure 2 illustrates the spatial distribution of summer mean precipitation during the period of 1989–2007. According to the observation data, the strong precipitation mainly occurs over the Changjiang-Huaihe valley and parts of Northeast China, and particularly in South China, where the summer mean precipitation reaches 8–10 mm/day. On the other hand, it is dry in the northern and western parts of China in summer. As shown in Fig. 2, the models overall capture well the main spatial patterns of precipitation in summer, such as the main rainbelt over the Changjiang-Huaihe valley and South China. However, there are large differences between the models. The simulated levels of precipitation by both RegCM4-CLM and RSM-NOAH are generally less than those of WRF-CLM and WRF-NOAH. Compared to the observations, the rainbelt in South China is underestimated by the former two models, while overestimated by the latter in intensity and magnitude. On the other hand, the rainbelt over Changjiang-Huaihe valley is shifted to the north in simulations by RegCM4-CLM and RSM-NOAH. It is worth noting that the spatial pattern of precipitation is similar between WRF-NOAH and WRF-CLM, which decreases by latitude from south to north, due to the two models using the same dynamical frame and physical process parameterization schemes (See

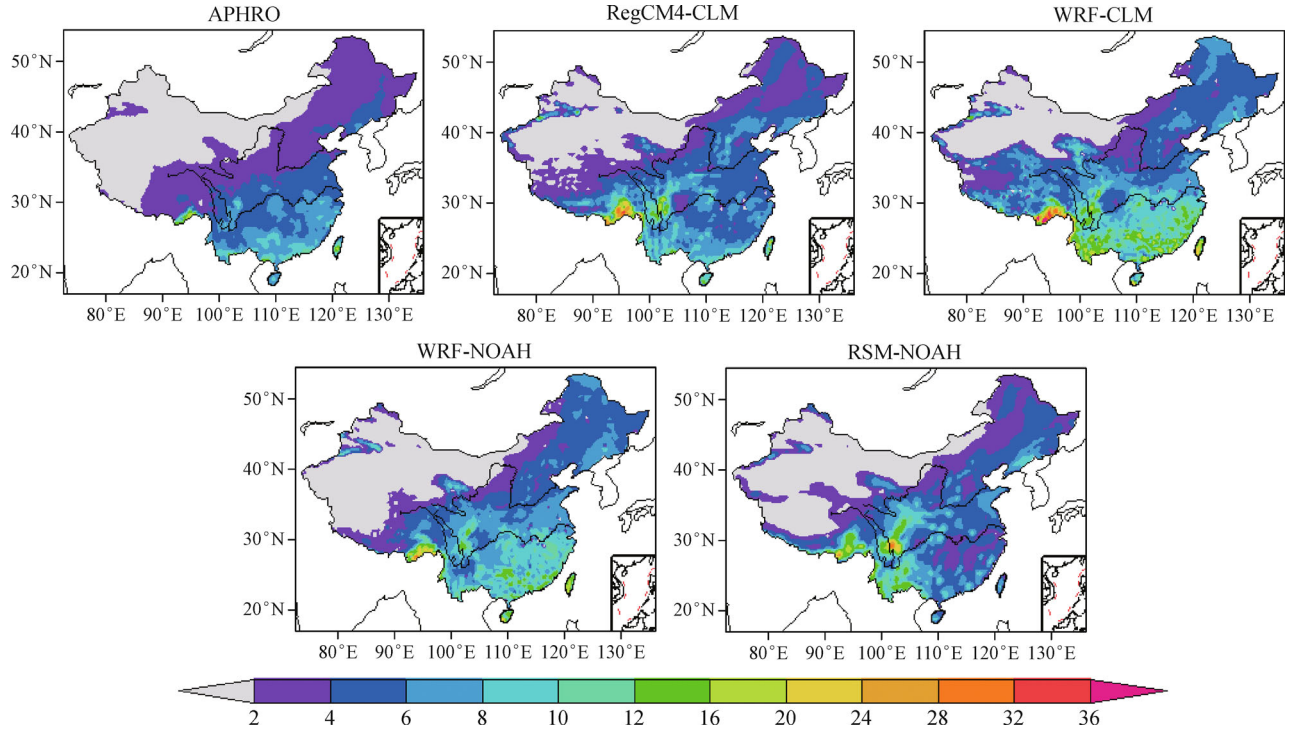

Fig. 2 The spatial distribution of summer mean precipitation for the period 1989–2007 (mm/day).

Table 1). However, the WRF-CLM precipitation result is generally greater over South China. The difference is mainly induced by the land surface process.

Observed precipitation shows a number of topographically induced, fine scale regional features, i.e., to the southeast of the Tibetan Plateau, over the Qilian mountains and the Tianshan mountains. The models successfully reproduce the strong precipitation around mountain areas in summer. However, the simulated intensity is greater than the observed intensity, especially in the southeastern Tibetan Plateau, where the RSM-NOAH model simulates a pseudo center of strong precipitation. The overestimate of precipitation over some of the topographical chains in the warm season is also documented by other researchers (Giorgi et al., 2004; Feng and Fu, 2006).

Figure 3 shows the spatial distribution of normalized bias of the summer precipitation for four models. The normalized bias is defined as the simulations relative to the observations (%). The western part of China overall has the largest bias. The notable positive bias exists over most areas of Northwest China and surrounds the Tibetan Plateau, where the largest bias exceeds 100% for the four models. Negative bias occurs over the Tarim and Junggar Basin. Due to the few observation stations in the western part of China, a large bias may exist in the observation dataset. Han and Zhou (2012) found that the observational dataset agrees with the stations' data in climate mean states, but underestimates precipitation intensity in the Yangtze River Basin and overestimates precipitation frequency over the western part of China. Therefore, the deficiency of data is one of the possible reasons for the overall large biases in the western part of China. The large differences also exist over South China, where the WRF-CLM and WRF-NOAH models overestimate precipitation by about 50%, while the RegCM4-CLM and RSM-NOAH underestimate by about 40%. In general, the WRF-CLM simulates the largest amount of precipitation, while the RSM-NOAH simulates the least among the four models. The model performance for summer mean precipitation in this study agrees with other model results (Fu et al., 2005; Feng and Fu, 2006, 2007; Gao et al., 2011; Wang and Sun, 2013).

Figure 4 shows the 850 hPa wind fields and moisture flux for the 19-year summer mean simulations. On the East Asian continent, the southwestern and southeastern monsoons prevail in the summer time, which transport abundant water vapor northward from the Bay of Bengal and the Western Pacific, respectively. The monsoon brings plentiful precipitation to South China, then to Changjiang-Huaihe, and later to North China. The simulated flow and moisture flux are generally comparable with other model results (Feng and Fu, 2006; Zhao, 2013). The four models all simulated the westerly winds over the Indian subcontinent and the southwesterly flow in southeast China, as well as in the East China Sea and Japan. However, obvious bias exists between the models. The WRF-CLM and WRF-

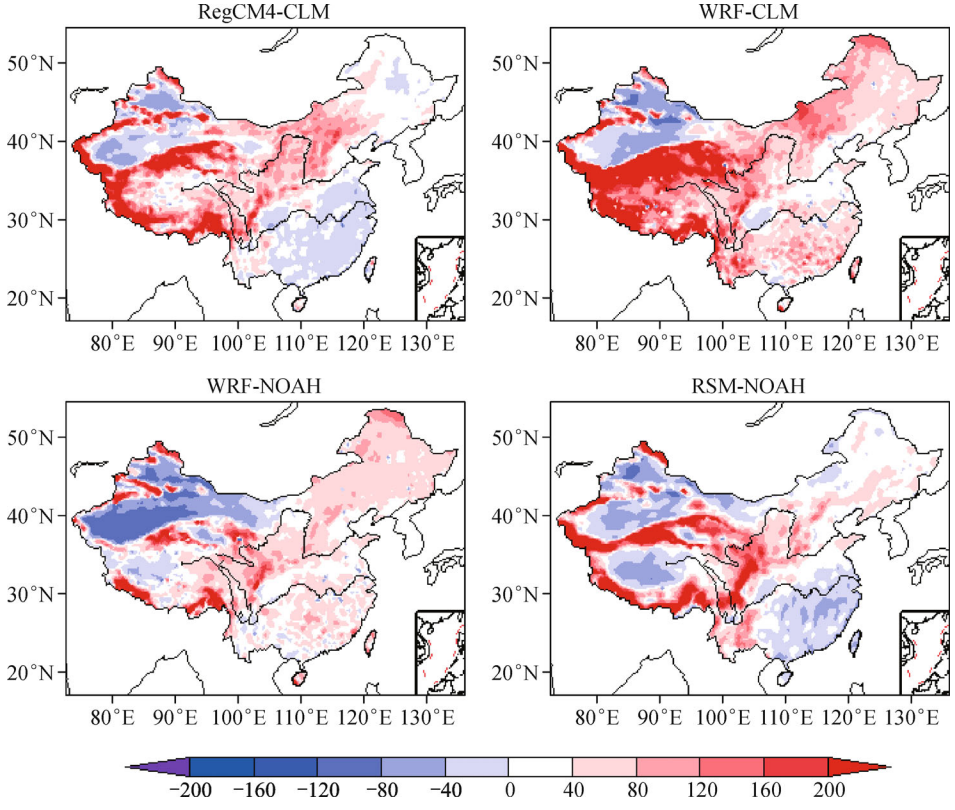

Fig. 3 Normalized bias (%) of summer precipitation for the period 1989–2007.

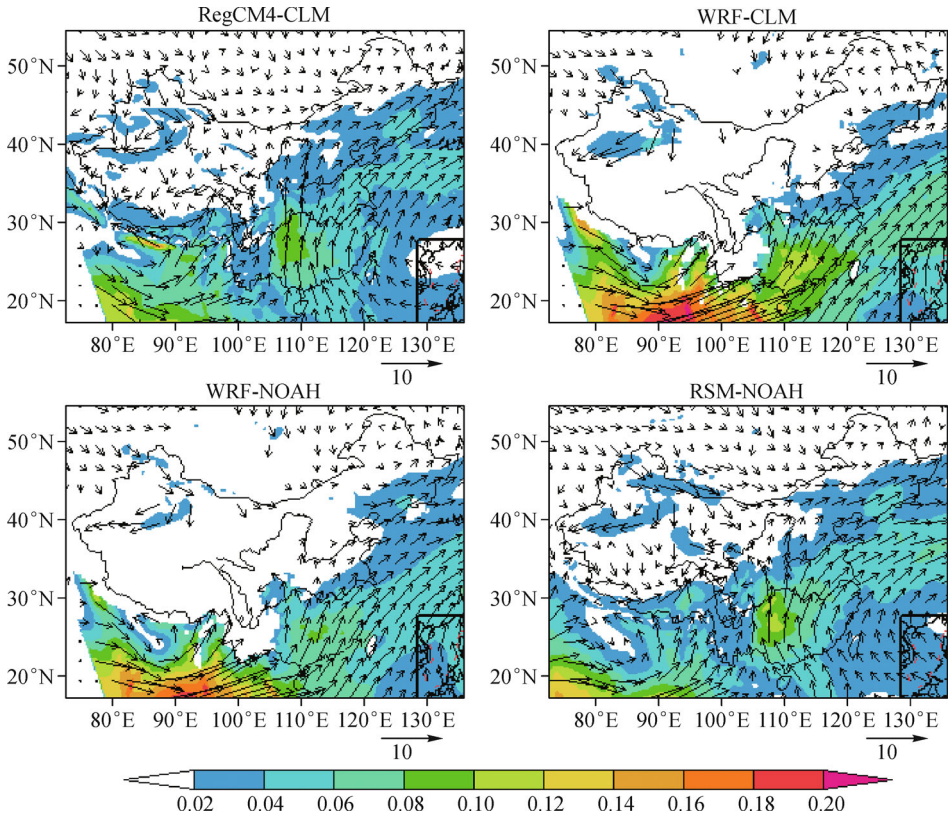

Fig. 4 The simulated spatial distributions of wind (m/s, vectors) and moisture flux (g/(cm·s), shaded) at 850 hPa in summer for the period 1989–2008.

NOAH simulated southwesterly flows are much stronger and shift to the south, with weaker westerly winds in the low latitudes than the other two models. Therefore, the simulated transferred southerly winds from the South China Sea to middle China are weaker, but to the southeast are stronger. This corresponds to a weaker southeasterly monsoon but a stronger southwesterly monsoon by WRF-CLM and WRF-NOAH. For moisture transport at 850 hPa, the WRF-CLM and WRF-NOAH simulated much stronger moisture flux transport from the northern part of the southwesterly flow from the Bay of Bengal to the central part of eastern China, which has a significant effect on the precipitation simulations for both the location and intensity. As a result, the precipitation is overestimated in southeast China by WRF-CLM and WRF-NOAH. As discussed above, the main difference between the four models lies in the more strongly simulated southwesterly flow and moisture flux transported to southeast China by WRF-CLM and WRF-NOAH, with the weaker moisture flux in the western Pacific by RegCM4-CLM and RSM-NOAH. This is the main reason for the simulated precipitation bias of RCMs in the summer.

Overall, the models successfully simulated the main spatial patterns of the summer mean surface air temperature over China during the 20-year period of 1989–2008 (Fig. 5). The models capture well the south-north gradient in temperature and also the topographically induced regional detail, which is of the same scale in the observations and simulations. Similar to the observations, the simulated temperature gradually decreases by latitude in the eastern part of China, where the terrain is flat. Due to the complex terrain conditions over the western part of China, there is obviously a temperature gradient in the areas where the terrain is steep. A cold center occurs in Tibetan Plateau both in observations and simulations, while it is warm in the Tarim, Junggar, and Sichuan Basins. The models also capture well the cold temperatures induced by small mountains, such as the Tianshan and Qilian mountains. In general, the WRF-CLM appears characterized by a predominant warm bias of a few degrees, while a small cold bias exists in RSM-NOAH and more mixed biases are found in RegCM4-CLM.

As shown in Fig. 6, the normalized bias has obvious differences between the models. Over the north of the Changjiang-Huaihe valley, the RegCM4-CLM and WRF-NOAH models simulate negative bias, while the WRF-CLM and RSM-NOAH results are positive. In South China, the models have a negative bias except for WRF-CLM. All the models show large cold bias along the Kunlun Mountains and the Himalayas in the west. Overall, the bias is larger in the west of China than in the east for all the models. Two factors could be adduced to explain the

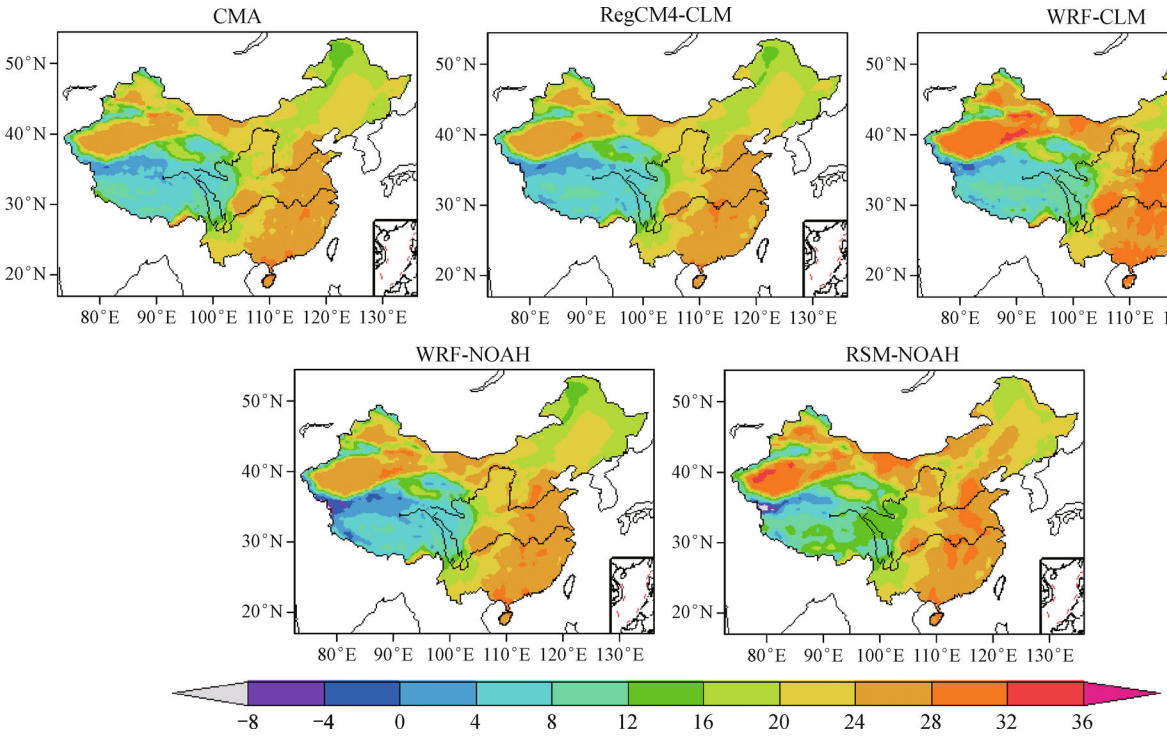

Fig. 5 The spatial distribution of summer means surface air temperature (°C) for the period 1989–2008.

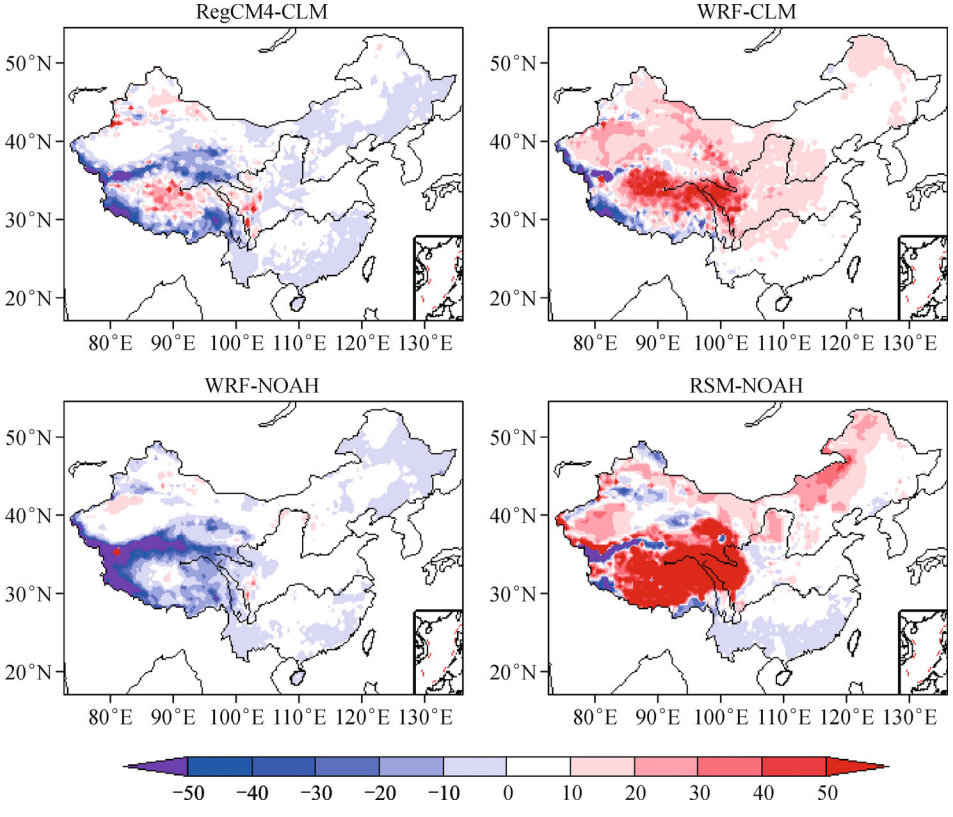

Fig. 6 Normalized bias (%) of summer temperature for the period 1989–2008.

large bias over the western areas. First, the stations are sparse, so the uncertainties of the observational data may be larger in this region (Xu et al., 2009). Second, the bias may be attributed to the complex terrain, which reduced the model performance in temperature. For all of the models, the normalized bias achieves −50% (−8°C) to −30% (−4°C) along the Kunlun Mountains and the Himalayas, while less than ±20% (2°C) over the east part of China. In contrast, the RSM-NOAH model has an obviously warm bias by 30%−50% (4°C−8°C) over the Tibetan Plateau, this bias may be caused by the model physics parameterization. In general, the model performance for temperature over China is comparable to other model results (Fu et al. 2005; Feng and Fu, 2007; Zhang et al., 2007; Gao et al., 2011; Hu and Wang, 2011).

The simulated precipitation and temperature bias, and the temporal and spatial correlations in every sub-region are statistically computed and shown in Table 2 and Table 3. The model bias is defined as the difference between the 19 year (20 year) summer average simulated precipitation (temperature) and the observational dataset.

All the models overestimate the summer mean precipitation in Northeast, North, and Northwest China, while underestimate it in South China (Table 2). In the Yangtze River Basin, the WRF-CLM and WRF-NOAH have a positive bias of 1.7 mm/day and 1.6 mm/day, respectively. However, the RegCM4-CLM and RSM-NOAH results show a negative bias of 0.3 mm/day and 0.6 mm/day, respectively. Due to the large amount of precipitation in the Yangtze River Basin (5.5 mm/day) and South China (7.2 mm/day), though the bias is larger than the other three regions, the relative difference is smaller. Overall, the WRF-CLM and WRF-NOAH systematically simulate greater precipitation than the other two models. For temporal correlations, the WRF-CLM (0.76) and WRF-NOAH (0.68) results are obviously better than that of RegCM4-CLM (0.18) and RSM-NOAH (−0.22) in Yangtze River Basin, while the RSM-NOAH results are worst in North and South China. On the other hand, the temporal correlations are comparable in Northeast (0.55−0.73) and Northwest China (0.57−0.67) among the four models.

Due to the complex terrain over China, the precipitation and temperature not only vary in temporal, but also have obviously large difference in spatial correlations. The spatial correlation could partly reflect the model performance for the spatial pattern of precipitation and temperature. As can be seen in Table 2, the spatial correlations simulated by WRF-CLM (0.54) and WRF-NOAH (0.50) are much higher than that of RegCM4-CLM (0.14) and RSM-NOAH (−0.24) in Yangtze River Basin, while the correlations are comparable with the models in other subregions. Overall, the simulated spatial correlations are higher in dry regions (Northeast (0.71−0.87), North (0.50−0.77), and Northwest China (0.71−0.83)) than that of wet regions (Yangtze River Basin (−0.24−0.54) and South China (0.15−0.31)).

All the models show positive bias for temperature over most areas of the domain, except for WRF-NOAH results in Northeast (−0.3°C) and Northwest (−0.1°C) China,

Table 2 The bias, temporal and spatial correlations for summer mean precipitation between the simulations and observations dataset during the period 1989−2007 in subregions

	Northeast China			North China			Yangtze River Basin			South China			Northwest China		
	Bias	Temp. R	Spatial R	Bias	Temp. R	Spatial R	Bias	Temp. R	Spatial R	Bias	Temp. R	Spatial R	Bias	Temp. R	Spatial R
OBS		3.0			3.0			5.5			7.2			0.7	
RegCM4-CLM	0.7	0.70	0.71	1.1	0.41	0.50	−0.3	0.18	0.14	−3.0	0.56	0.31	0.6	0.63	0.76
WRF-CLM	2.0	0.55	0.76	0.9	0.58	0.61	1.7	0.76	0.54	−0.3	0.58	0.15	1.2	0.58	0.71
WRF-NOAH	1.8	0.73	0.87	0.8	0.61	0.77	1.6	0.68	0.50	−1.1	0.63	0.20	0.2	0.67	0.83
RSM-NOAH	0.6	0.60	0.87	0.9	−0.07	0.63	−0.6	−0.22	−0.24	−3.3	0.25	0.24	0.4	0.57	0.73

Table 3 The bias, temporal and spatial correlations for summer mean near surface temperature between the simulations and observations dataset during the period 1989−2008 in subregions

	Northeast China			North China			Yangtze River Basin			South China			Northwest China		
	Bias	Temp. R	Spatial R	Bias	Temp. R	Spatial R	Bias	Temp. R	Spatial R	Bias	Temp. R	Spatial R	Bias	Temp. R	Spatial R
OBS		19.3			22.4			25.1			26.0			16.8	
RegCM4-CLM	0.0	0.85	0.96	0.3	0.46	0.96	0.3	0.60	0.95	0.4	0.60	0.93	0.2	0.84	0.99
WRF-CLM	1.2	0.81	0.95	2.1	0.76	0.95	2.3	0.67	0.92	1.8	0.56	0.93	2.7	0.77	0.99
WRF-NOAH	−0.3	0.95	0.96	1.0	0.68	0.96	0.5	0.72	0.97	0.8	0.64	0.98	−0.1	0.79	0.99
RSM-NOAH	2.4	0.83	0.64	1.6	0.55	0.80	0.9	0.57	0.93	0.6	0.28	0.91	2.1	0.65	0.95

which have small negative bias (Table 3). Among the four models, the WRF-CLM (1.2°C−2.7°C) simulated bias is the largest, while the RegCM4 (0.0°C−0.4°C) result is the best. All the models well simulate both the temporal and spatial correlations for temperature in all subregions, which are rather better than that of precipitation, implying that the model performance is better for temperature than for precipitation.

3.2 Interannual variability

Figure 7 shows the interannual variations of precipitation and temperature in five subregions in summer. The increase of climate variability has important societal and economic impacts since it is difficult to adapt to changes in extremes (Giorgi et al., 2004; Duffy et al., 2006). The values of interannual variation were computed by first calculating the anomaly at each grid cell and then averaging it over all the land grid points of the regions. As can be seen, most of the models can reasonably reproduce the interannual variation of the precipitation and temperature in all subregions. Using the 1989–2007 time period as a baseline, both the observations and simulations show large interannual variations in precipitation. For example, in Yangtze River basin, the observed precipitation indicates that certain years are drier (2005−2006) or wetter (1997–1998) than the 19-year summer mean climatological average. However, these wet and dry anomalies do not occur simultaneously in all subregions. In contrast, the observed precipitation is wetter (2005−2006) and drier (1997−1998) in South China, but the simulations are consistently like that in Yangtze River basin. However, there are large differences between the models in North China and Yangtze River Basin. Overall, the simulated interannual variation of the temperature is better than that of precipitation. The differences are smaller for temperature between the models. In Northeast and Northwest China, the simulations agree well with the observations. In general, the WRF-CLM and WRF-NOAH simulate better interannual variations of precipitation and temperature compared with observations from those of RegCM4-CLM and RSM-NOAH. The model performance for interannual variability in the warm season may be mainly affected by the local and mesoscale land surface and convective processes (Christensen et al., 2001; Giorgi et al., 2004; Steiner et al., 2009).

The temporal standard deviation was computed for each grid cell to describe the spatial pattern of interannual variability for precipitation and temperature. In summer, the primary source of interannual variability over China is the East Asian Summer monsoon, which affects precipitation by varying the amount of moisture advected into the region. The interannual variability of summer mean precipitation (Fig. 8) shows that locations of high interannual variability generally agree well with locations of high summer mean precipitation (Fig. 2). The models overall reproduce the observed spatial pattern of high interannual variability over the Yangtze River basin and South China, and low variability over the dry regions in the northwest and the Tibetan Plateau. In addition, the models well simulate the center of the larger variability over the mountains in Tianshan, Qilian, and the Himalayas. However, there are obvious differences between the models. In wet regions, the WRF-CLM and WRF-NOAH simulated interannual variabilities are greater than observations, while the RegCM4-CLM and RSM-NOAH results are smaller. In northern China (i.e., in the Tarim Basin of Xinjiang) and the Northeast, the simulated interannual variability is larger than observations.

The observed interannual variability of summer-mean near-surface temperature is higher in north China, especially in the east of Inner Mongolia, and decreases gradually from north to south by latitude (Fig. 9). The RegCM4-CLM and WRF-CLM models can well reproduce the spatial distribution and magnitude of the interannual variability. The WRF-NOAH simulated interannual variability coincides with observations in the eastern part of China, but is higher in the Tibetan Plateau. The RSM-NOAH simulates excessive variability in the Tibetan Plateau, the Northeast, and the Yangtze River Basin, which coincide with locations of large temperature bias (Fig. 6).

3.3 Trends

In this section, the simulated climatic trends of summer precipitation and temperature are compared to the observations. The linear trend is defined as a least square fit line to the 19 (20) years of the precipitation (temperature). A good model performance for climatic trends can also enhance the confidence in the model's ability for internal variability (Giorgi et al., 2004). The spatial distribution of the linear trend of observed and simulated summer precipitation during the period 1989–2007 is shown in Fig. 10. The observation illustrates a negative trend (drying) over Northeast and Northwest China, and the Yangtze River basin, with a positive trend (wetting) over North and South China. All the models well capture the dominantly negative trends over the northern part of China except for WRF-CLM, which gives a larger negative trend in the Yangtze River basin and shifts to the north. The models agree with the positive trend over South China except for RSM-NOAH, which simulates an almost negative trend over China. On the other hand, the positive trends are better simulated by WRF-CLM and WRF-NOAH, implying that they are essentially controlled by the model dynamics. Overall, the RegCM4-CLM best simulates the spatial pattern and magnitude of the linear trend for summer precipitation.

Figure 11 shows the observed and simulated near surface air temperature linear trend during the period 1989–2008. The observed temperature trend is positive

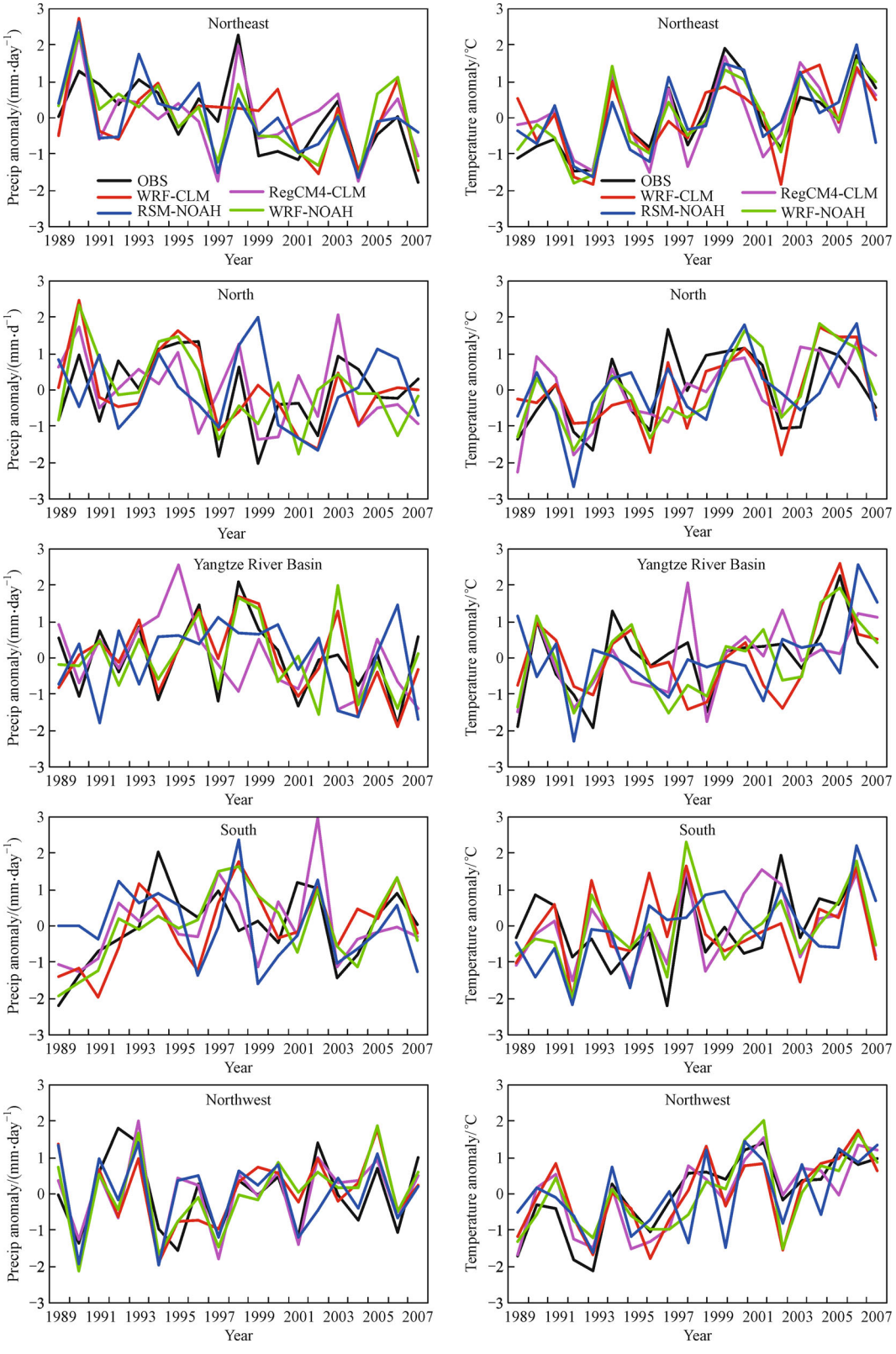

Fig. 7 Interannual variations of summer means precipitation (left column) and temperature (right column) averaged over the 5 subregions of Fig.1.

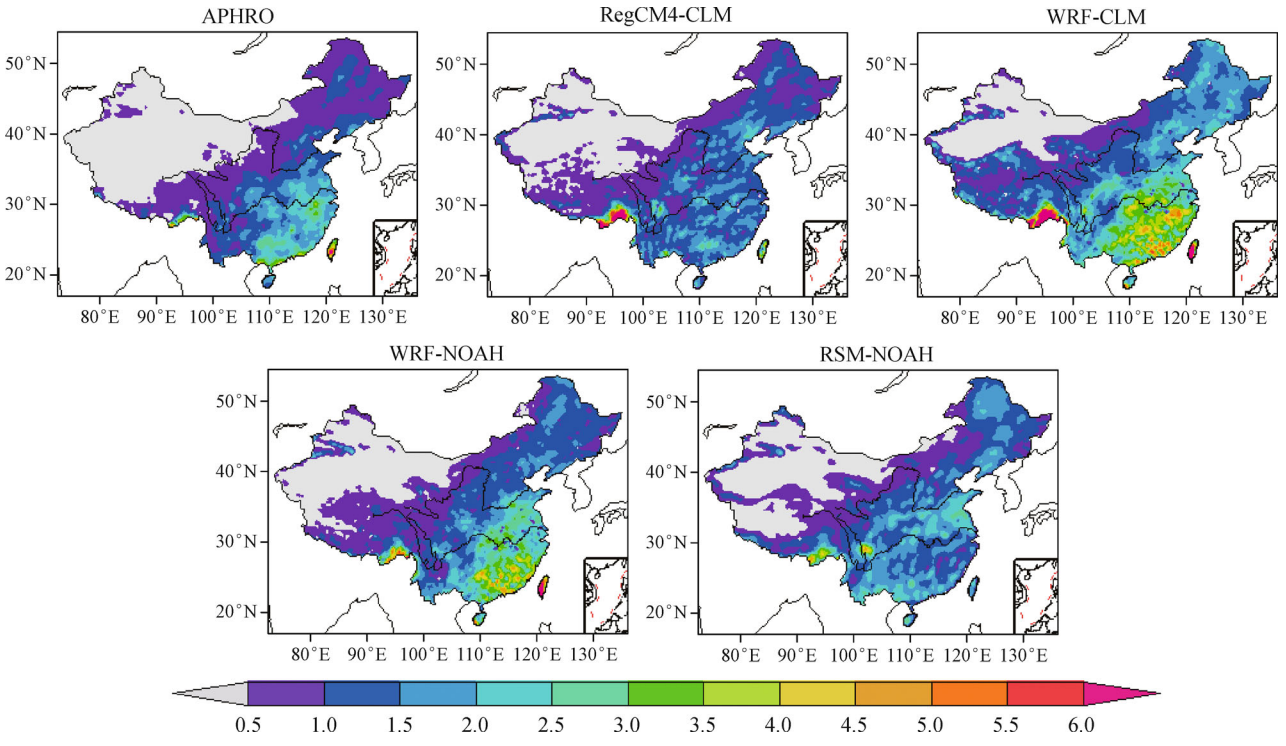

Fig. 8 Interannual variability of summer means precipitation (mm/day).

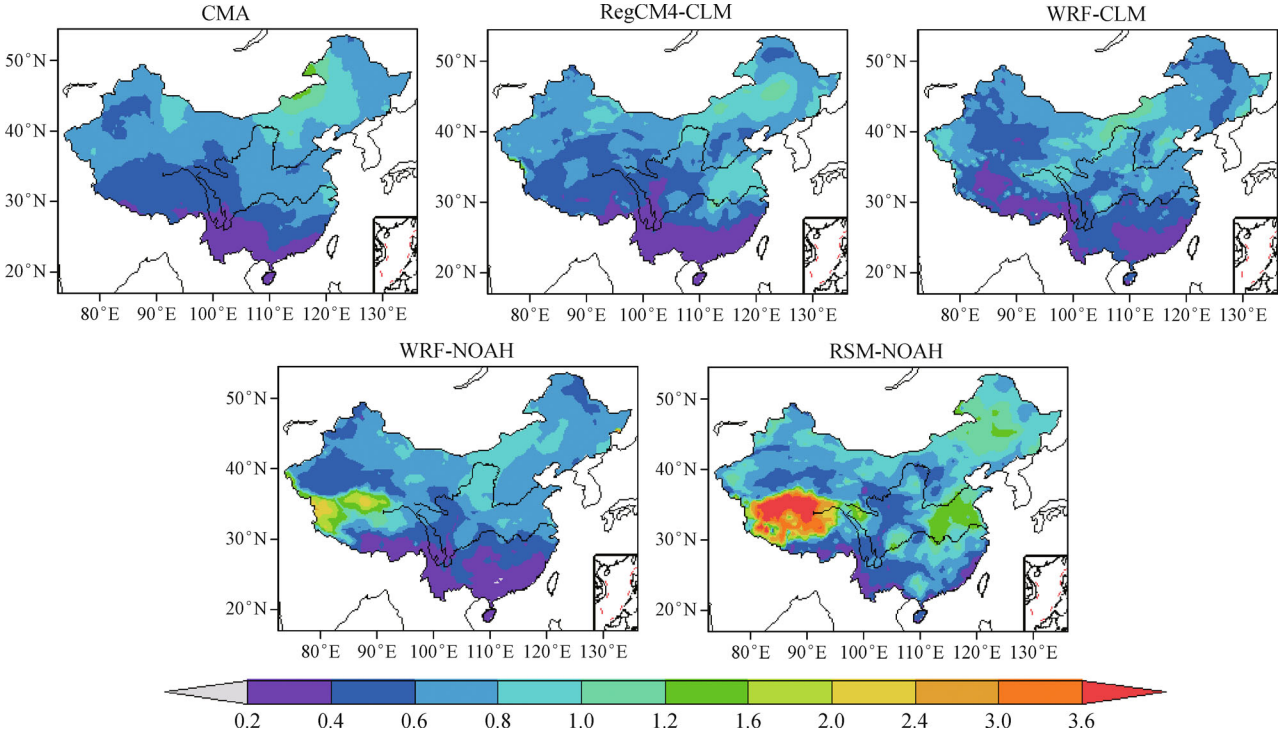

Fig. 9 Interannual variability of summer means surface air temperature (°C).

over Northeast China and the western part of China, including Xinjiang, Qinghai, and Gansu, while in other regions, the trend is small. Similar to the observations, all the models simulate a positive trend over the northern part of China, but the spatial patterns are different, i.e., the trend simulated by WRF-CLM is smaller over the Northeast but

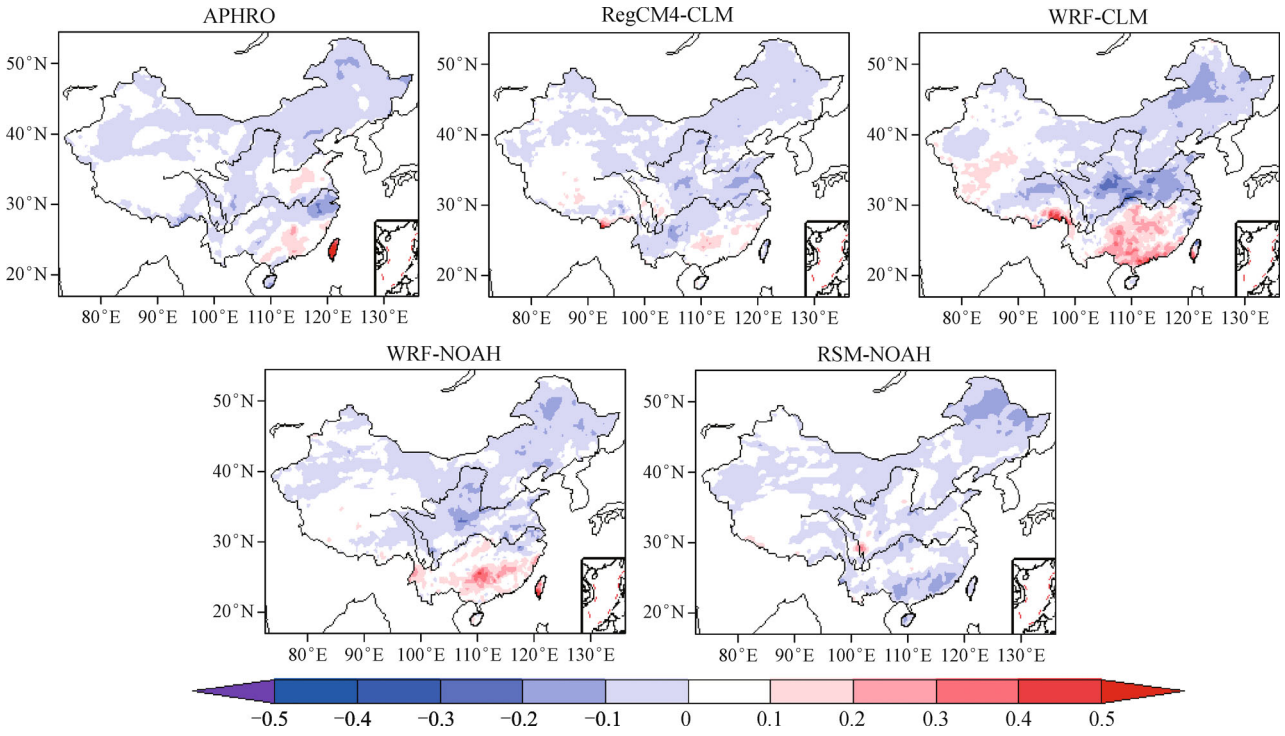

Fig. 10 Linear trend of summer time precipitation for the period 1980−2008 (mm/day/decade).

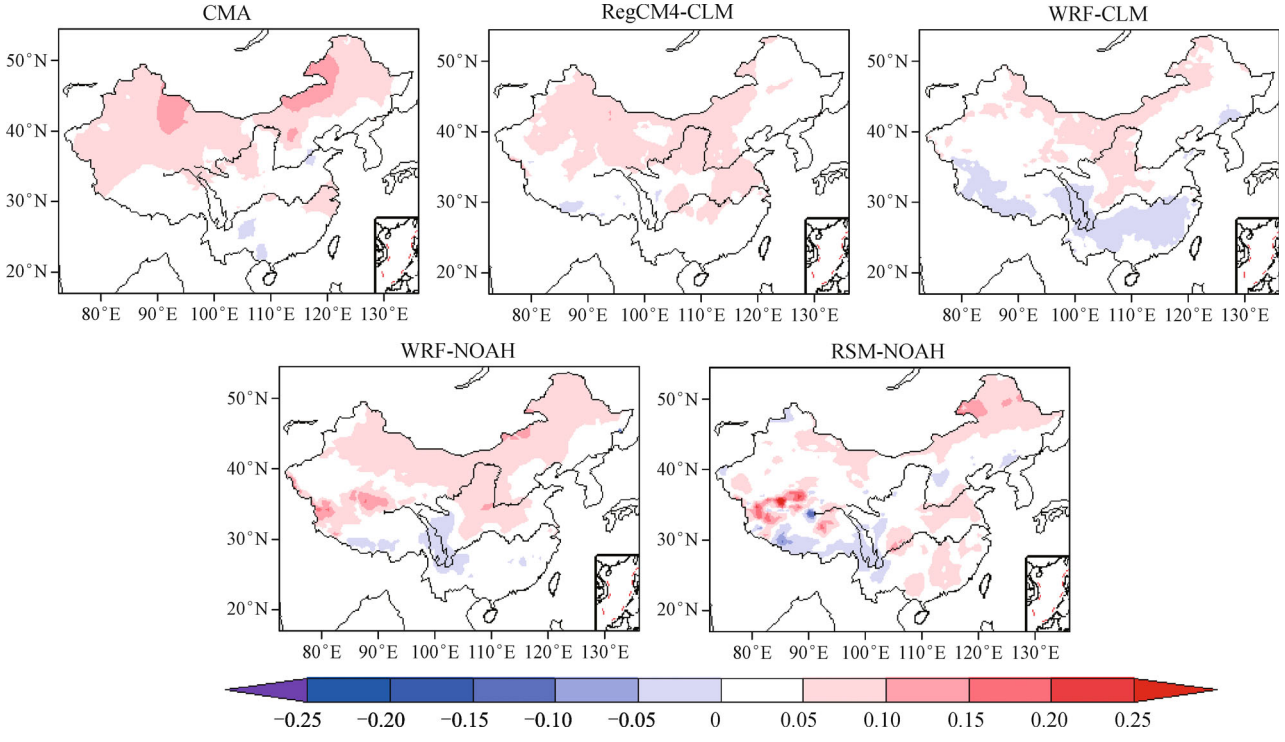

Fig. 11 Linear trend of summer time near surface air temperature for the period 1980−2008 (°C/decade).

larger in Ningxia and Shaanxi, while the trend simulated by RSM-NOAH is smaller over the western part of China. Over South China, WRF-CLM predicts a small negative trend, while RSM-NOAH is positive; the other two models simulate relatively small positive trends, which agree well with the observations.

3.4 Extremes

Climate extremes have large negative impacts on society and ecosystems. Analysis of simulated climate extremes can lead to better understanding the model performance and is useful to estimate the future changes in the frequency and intensity of extreme events over China, under the background of global warming. The indices of heavy rain days R25 (identified as the number of days with precipitation lager than 25 mm/day in summer) and heavy precipitation fraction R95t (identified as the fraction of the summer total precipitation due to events exceeding the 1989–2007 95th percentile %) are selected to identify the summer time extreme precipitation, while $T_{2\max}$ (daily maximum temperature at 2 m height) and $T_{2\min}$ (daily minimum temperature at 2 m height) are used for extreme temperatures.

3.4.1 Extreme precipitation

The observed R25 shows that heavy precipitation mainly occurs over South China and Changjiang-Huaihe valley, and the R25 value is about 6–10 days in summer over these areas (Fig. 12). Overall, the models generally well capture the special characteristics of R25, i.e., larger in the southeastern coast but smaller inland, to the northwest. The simulated R25 has a pseudo large center in the eastern part of the Tibetan Plateau corresponding to the numerical point storms, especially for the RSM-NOAH model. This problem was also found for all the earlier models, in which a false heavy precipitation center was always simulated in the eastern Plateau (Feng and Fu, 2006; Jiang et al., 2012). Also, the simulated R25 is larger than observations over the Qilian and Tianshan mountains. For the subregions, both the observed and simulated R25 are small in Northwest China. In Northeast and North China, the models overestimate R25 by 2–4 days for WRF-CLM and WRF-NOAH, and 1–3 days for RegCM4-CLM and RSM-NOAH. In the Yangtze River Basin and South China, the WRF-CLM and WRF-NOAH overestimate R25 by 4–6 days while RegCM4-CLM and RSM-NOAH underestimate R25 by 2–3 days.

Figure 13 displays the spatial distribution of observed and simulated heavy precipitation fraction (R95t). The observation shows that R95t is about 20%–28% over the eastern monsoon region of China, while about 10%–15% over the western part of China in summer. The models well simulate the special patterns of R95t. In the western part of China, the simulated R95t is close to observations since the heavy precipitation events are rare. However, in the Tarim Basin, the WRF-NOAH simulated R95t is obviously lower than observations. In the eastern part of China, the WRF-CLM and WRF-NOAH simulated R95t is slightly larger than observation by 2%–4%. On the other hand, the RegCM4-CLM simulated R95t is about 8% higher than observations over the Yangtze River Basin and North China. RSM-NOAH is 4% lower over North China and 4%–8% lower over the northeastern and southeastern parts of China.

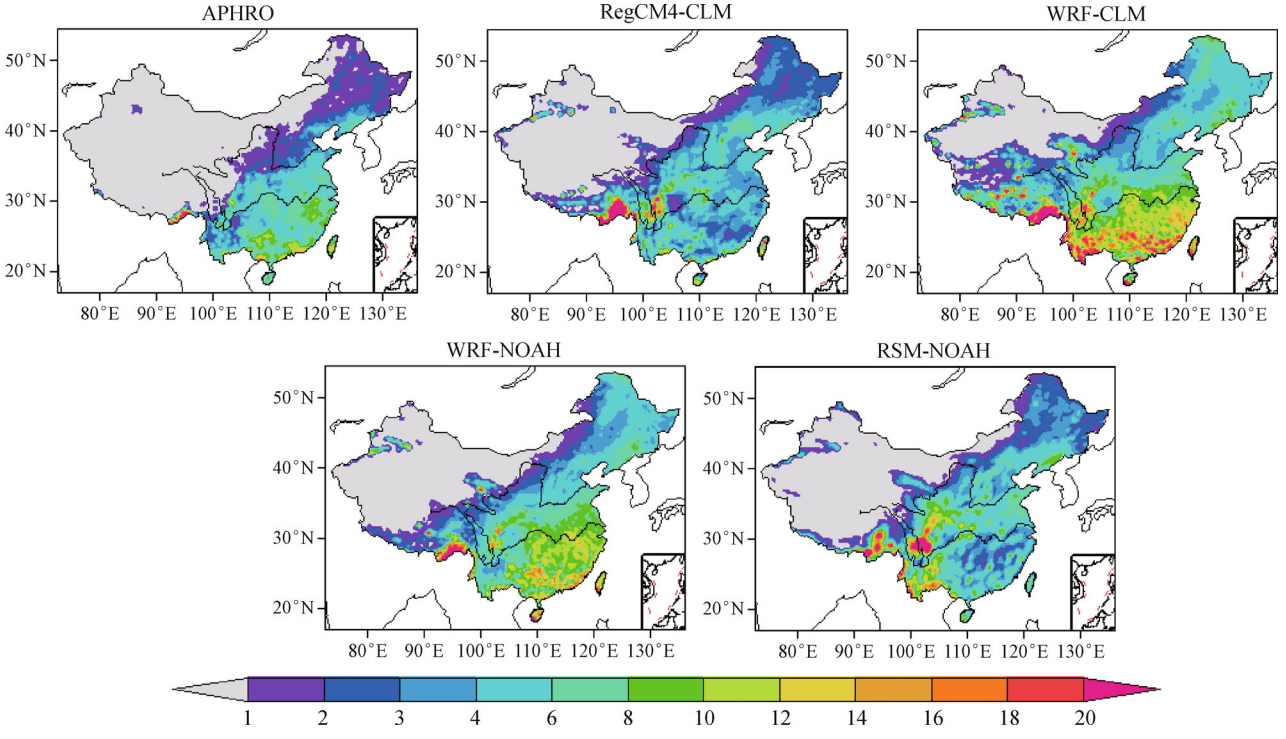

Fig. 12 Special distribution of heavy rain days (R25) for the period 1980–2007.

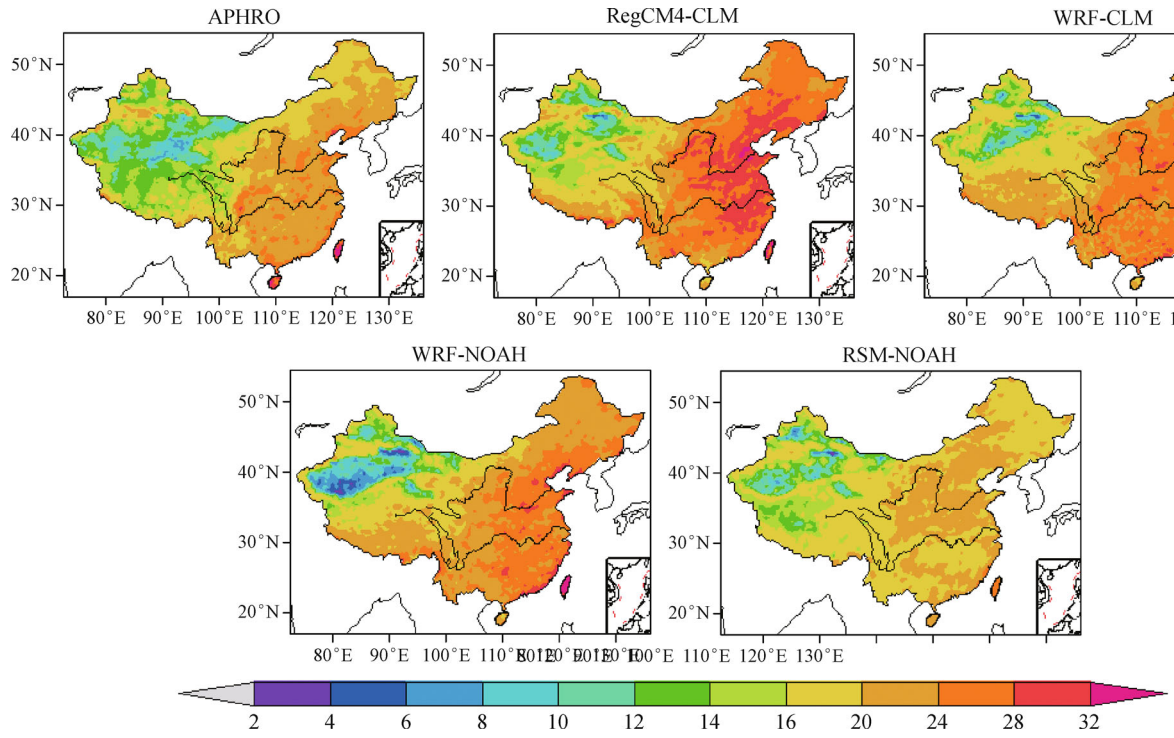

Fig. 13 Special distribution of heavy precipitation fraction (R95t) for the period 1980–2007.

3.4.2 Minimum and maximum temperatures

Figure 14 shows the observed and simulated summer means T_{2max} and T_{2min} over China during 1989–2008. The observed T_{2max} shows a warm center in the Tarim Basin and a cold center in the Tibetan Plateau. The models can well reproduce the observed spatial pattern of T_{2max}. The magnitude of T_{2max} is well simulated by RegCM4-CLM, while the WRF-CLM has a warm bias of 2°C–5°C over the Tarim Basin and the eastern part of China. The WRF-NOAH result shows a similar pattern to WRF-CLM, but the warm bias is smaller. The RSM-NOAH model systematically underestimates the T_{2max} over most part of China for 3°C–6°C.

The summer mean T_{2min} spatial distribution is similar to T_{2max}. The general spatial patterns are reproduced by the models, though there are some large differences. The WRF-CLM result has a warm bias of 2°C–4°C over southern China, the Tarim Basin, and the Tibetan Plateau. The WRF-NOAH result is similar to the observations but colder on the Tibetan Plateau. By contrast to T_{2max}, the RSM-NOAH seems to systematically overestimates the T_{2min} over China by 2°C–5°C.

In general, the RegCM4-CLM ability to simulate T_{2max} and T_{2min} is the best, while the RSM-NOAH is the worst among the four models. Compared to mean temperatures (Fig. 5), the differences between models and observations are larger for T_{2max} and T_{2min}.

4 Discussion and conclusions

A 20-year summer time simulation during the periods of 1989–2008 for the regional climate of China is conducted by four regional climate models coupled with land surface models. Model performance is evaluated by comparing their simulations of the means, interannual variability, trends, and extremes of precipitation and temperature with observations. The daily mean precipitation data during the period 1989–2007 and the daily mean, maximum, and minimum near surface temperature data during the period 1989–2008 are used for model comparison.

Overall, most of the models can reasonably simulate the spatial pattern of summer mean precipitation and temperature. However, there are obviously differences between the observations and model results. The WRF-CLM and WRF-NOAH models which use the Kain-Fritsch convection scheme overestimate the precipitation in most continental regions. Furthermore, the land surface process has a large influence on the precipitation simulation. For temperature, the models well reproduce the south to north gradient over the eastern part of China, and the warm center in Tarim, Junggar, and Sichuan Basin in the west. It is important to emphasize that all the models captured well the topography-induced summer time precipitation and near surface temperature at the resolution considered.

Further analysis within the five subregions shows that the model generally captures the rain belt in South China

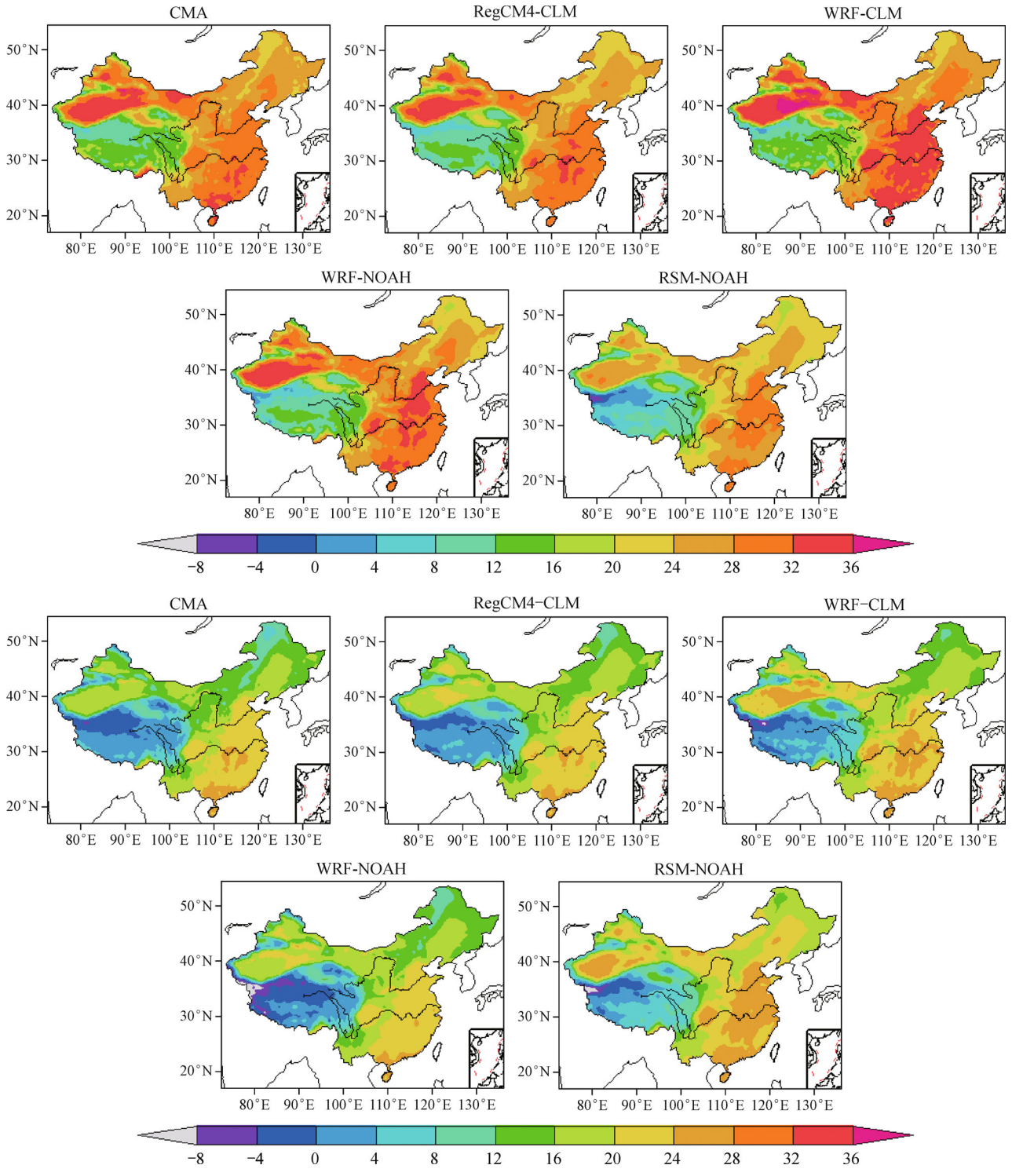

Fig. 14 The observed and simulated summer means T_{2max} and T_{2min} during 1989−2008 (the top is T_{2max}, and the bottom is T_{2min}).

and the Yangtze River Basin, which are closely connected with the East Asia monsoon rain belt movement in the Indo-China Peninsula. In general, all the models overestimate the precipitation in Northeast, North, and Northwest China, while underestimate precipitation in South China. In the Yangtze River Basin, the WRF-CLM and WRF-NOAH have a positive bias, but the RegCM4-CLM and RSM-NOAH model results are negative. In terms of the temporal and spatial correlations of precipitation, all the models perform well in the dry regions. The WRF-CLM and WRF-NOAH results are obviously better than RegCM4-CLM and RSM-NOAH in the wet regions. The

temperature biases are generally less than ±20% (2°C) in all subregions. All the models overestimate the temperature over most of the domain, except for WRF-NOAH in Northeast and Northwest. The good temporal and spatial correlations indicate that the simulations agree well with the observations. Overall, the WRF-CLM and WRF-NOAH models simulate warmer and wetter, while RegCM4-CLM and RSM-NOAH simulate colder and dryer climate over large areas of China. The model performance is better for temperature than for precipitation.

The models can generally capture the major anomalies in interannual variation of precipitation and temperature in all subregions. Overall, the simulated interannual variation of the temperature is better than that of precipitation for all models. The WRF-CLM and WRF-NOAH both produce the interannual variation of precipitation and temperature with higher fidelity than either that of RegCM4-CLM and RSM-NOAH. The models reproduce well the observed spatial pattern of high interannual variability for precipitation over wet regions, and low variability over the dry regions. The WRF-CLM and WRF-NOAH show a tendency to overestimate interannual variability of precipitation over large areas of China. All the models, except for RSM-NOAH, capture well the spatial pattern and magnitude of interannual variability in the temperature gradient from south to north by latitude. The RSM-NOAH, however, simulates excessive variability in the Tibetan Plateau and the Yangtze River Basin, which coincide with locations of large temperature bias. As discussed by Christensen et al. (2001), land surface and convective processes evidently play an important role in regulating the simulated interannual variability of warm season surface climate.

Most of the models can basically simulate the dominantly negative linear trend of precipitation over large parts of China. Noticeably, the models capture the drying trend over the Yangtze River Basin and the increasing precipitation trend over South China, though the areas and magnitude differ from the observations. The models reasonably simulate the increasing linear trend of temperature over the north part of China, and a relatively small negative trend in some areas. However, there are differences between the models and observations, especially over South China. It is worth noting that the precipitation and temperature trends are small and not statistically significant in this study; further studies are necessary to yield a more robust conclusion on this issue.

The models generally capture the sign and magnitude of heavy rain days (R25). The large value of R25 occuring in South China and the Changjiang-Huaihe valley correspond to high precipitation in summer in these areas. The observed and simulated heavy precipitation fraction (R95t) are close to each other in the western part of China due to the rare heavy precipitation events. On the other hand, the WRF-CLM and WRF-NOAH simulate well the R95t, while the RegCM4-CLM is higher and RSM-NOAH is lower than observations in the eastern part of China.

The models capture well the spatial pattern and magnitude of the daily maximum and minimum temperatures over China. The RegCM4-CLM ability to simulate $T_{2\max}$ and $T_{2\min}$ is the best, while the RSM-NOAH is the worst among the four models. The differences between models and observations are larger for $T_{2\max}$ and $T_{2\min}$ than that of mean temperature.

Acknowledgements This work was supported by the National Basic Research Program of China (No. 2011CB952004), and the National Natural Science Foundation of China (Grant Nos. 41305006, 41375075, and 91425304). The numerical calculations in this paper have been done on the IBM Blade cluster system in the High Performance Computing Center (HPCC) of Nanjing University.

References

Chen F, Manning K W, LeMone M A, Trier S B, Alfieri J G, Roberts R, Tewari M, Niyogi D, Horst T W, Oncley S P, Basara J B, Blanken P D (2007). Description and evaluation of the characteristics if the NCAR high-resolution land data assimilation system. J Appl Meteorol Climatol, 46(6): 694–713

Chen W L, Jiang Z H, Li L, Yiou P (2011). Simulation of regional climate change under the IPCC A2 scenario in southeast China. Clim Dyn, 36(3−4): 491–507

Christensen O B, Gaertner M A, Prego J A, Polcher J (2001). Internal variability of regional climate models. Clim Dyn, 17(11): 875–887

Collins W D, Bitz C M, Blackmon M L, Bonan G B, Bretherton C S, Carton J A, Chang P, Doney S C, Hack J J, Henderson T B, Kiehl J T, Large W G, McKenna D S, Santer B D, Smith R D (2006). The community climate system model version 3 (CCSM3). J Clim, 19 (11): 2122–2143

Dickinson R E, Errico R M, Giorgi F, Bates G T (1989). A regional climate model for the western United States. Clim Change, 15(3): 383–422

Dong S Y, Xu Y, Zhou B T, Shi Y (2015). Assessment of indices of temperature extremes simulated by multiple CMIP5 models over China. Adv Atmos Sci, 32(8): 1077–1091

Duffy P B, Arritt R W, Coquard J, Gutowski W, Han J, Iorio J, Kim J, Leung L R, Roads J, Zeledon E (2006). Simulations of present and future climates in the Western United States with four nested regional climate models. J Clim, 19(6): 873–895

Ek M B, Mitchell K E, Lin Y, Rogers E, Grunmann P, Koren V, Gayno G, Tarpley J D (2003). Implementation of Noah land surface model advancements in the National Centers for Environmental Prediction operational mesoscale Eta model. J Geophys Res, 108(D22): 8851

Feng J M, Fu C B (2006). Inter-comparison of 10-year precipitation simulated by several RCMs for Asia. Advances in atmospheric sciences, 23: 531–542 (in Chinese)

Feng J M, Fu C B (2007). Inter-comparison of long-term simulations of temperature and precipitation over China by different regional climate models. Chinese Journal of Atmospheric Sciences, 32: 805–

814 (in Chinese)

Feng J M, Wang Y L, Fu C B (2011). Simulation of extreme climate events over China with different regional climate models. Atmospheric and Oceanic Science Letters, 2011, 4: 47–56

Fu C B, Wang S Y, Xiong Z, Gutowski W J, Lee D K, McGregor J L, Sato Y S, Kato H, Kim J W, Suh M S (2005). Regional climate model intercomparison project for Asia. BAMS, 257–266

Fu C B, Wei H L, Chen M (1998). Simulation of the evolution of summer monsoon rainbelts over eastern China from regional climate model. Chinese J Atmos Sci, 22(4): 522–534 (in Chinese)

Gao X J, Shi Y, Giorgi F (2011). A high resolution simulation of climate change over China. Sci China Earth Sci, 54(3): 462–472

Giorgi F (1990). Simulation of regional climate using a limited area model nested in a general circulation model. J Clim, 3(9): 941–963

Giorgi F, Bi X, Pal J S (2004). Mean, interannual variability and trends in a regional climate change experiment over Europe. I. Present-day climate (1961–1990). Clim Dyn, 22(6−7): 733–756

Giorgi F, Coppola E, Solmon F, Mariotti L, Sylla M B, Bi X, Elguindi N, Diro G T, Nair V, Giuliani G, Turuncoglu U U, Cozzini S, Güttler I, O'Brien T A, Tawfik A B, Shalaby A, Zakey A S, Steiner A L, Stordal F, Sloan L C, Brankovic C (2012). RegCM4: model description and preliminary tests over multiple CORDEX domains. Clim Res, 52: 7–29

Giorgi F, Marinucci M R, Bates G T (1993a). Development of a second generation regional climate model (RegCM2) I: boundary layer and radiative transfer processes. Mon Weather Rev, 121(10): 2794–2813

Giorgi F, Marinucci M R, Bates G T, de Canio G (1993b). Development of a second generation regional climate model (RegCM2) II: convective processes and assimilation of lateral boundary conditions. Mon Weather Rev, 121(10): 2814–2832

Giorgi F, Mearns L O (1999). Introduction to special section: regional climate modeling revisited. J Geophys Res, 104(D6): 6335–6352

Guo Y, Dong W J, Ren F M, Zhao Z C, Huang J B (2013). Surface air temperature simulations over China with CMIP5 and CMIP3. Adv Clim Change Res, 4(3), doi: 10.3724/SP.J.1248.2013.145

Han Z Y, Zhou T J (2012). Assessing the quality of APHRODITE high-resolution daily precipitation dataset over contiguous China. Chinese Journal of Atmospheric Sciences, 36(2): 361–373 (in Chinese)

Hong Y, Donat MG, Alexander LV, Sun Y (2014) Multi-dataset comparison of gridded observed temperature and precipitation extremes over China. International Journal of Climatoligy, doi: 10.1002/joc.4174

Hu B Y, Tang J P, Wang S Y (2012). A numerical simulation for mid-21st century climate change over China under IPCC A1B scenario. Journal of the Meteorological Sciences, 32(2): 127–136

Hu B Y, Tang J P, Wang S Y (2013). Evaluation and projection of extreme events over China under IPCC A1B scenario by MM5V3 model. Chinese J Geophys, 56(7): 2195–2206 (in Chinese)

Hu B Y, Wang S Y (2011). An assessment of surface air temperature and precipitation over China during 1982−2001 by regional climate model. Journal of Nanjing University(Natural Sciences), 47(3): 318–329

Jiang Z H, Song J, Li L, Chen W L, Wang Z F, Wang J (2012). Extreme climate events in China: IPCC-AR4 model evaluation and projection. Clim Change, 110(1−2): 385–401

Juang H M H, Hong S Y, Kanamitsu M (1997). The NCEP regional spectral model: an update. Bull Am Meteorol Soc, 78(10): 2125–2143

Kanamitsu M, Ebisuzaki W, Woollen J, Yang SK, Hnilo J J, Fiorino M, Potter G L (2002). NCEP-DOE AMIP-II Reanalysis (R-2). Bulletin of the American Meteorological Society, 83(11): 1631–1643

Katragkou E, Garcia-Diez M, Vautard R, Sobolowski S, Zanis P, Alexandri G, Cardoso R M, Colette A, Fernandez J, Gobiet A, Goergen K, Karacostas T, Knist S, Mayer S, Soares P M M, Pytharoulis I, Tegoulias I, Tsikerdekis A, Jacob D (2015). Regional climate hindcast simulations within EURO-CORDEX: evaluation of a WRF multi-physics ensemble. Geosci Model Dev, 8(3): 603–618

Liang X Z, Li L, Dai A, Kunkel K E (2004a). Regional climate model simulation of summer precipitation diurnal cycle over the United States. Geophys Res Lett, 31(24): L24208

Liang X Z, Li L, Kunkel K E, Ting M, Wang J X L (2004b). Regional climate model simulation of U.S. precipitation during 1982–2002. Part I: annual cycle. J Clim, 17(18): 3510–3529

Liang X Z, Xu M, Yuan X, Ling T, Choi H I, Zhang F, Chen L, Liu S, Su S, Qiao F, He Y, Wang J X L, Kunkel K E, Gao W, Joseph E, Morris V, Yu T W, Dudhia J, Michalakes J (2012). Regional climate–weather research and forecasting model. Bull Am Meteorol Soc, 93 (9): 1363–1387

Liu S Y, Gao W, Liang X Z (2013). A regional climate model downscaling projection of China future climate change. Clim Dyn, 41(7−8): 1871–1884

Oleson K W, Niu G Y, Yang Z L, Lawrence D M, Thornton P E, Lawrence P J, Stockli R, Dickinson R E, Bonan G B, Levis S, Dai A, Qian T (2008). Improvements to the Community Land Model and their impact on the hydrological cycle. J Geophys Res, 113(G1): G01021

Pal J S, Giorgi F, Bi X, Elguindi N, Solmon F, Gao X, Pauscher S A, Gao X , Francisco R, Zakey A, Winter J, Ashfaq M, Syed F S, Bell J L, Diffenbaugh N S, Karmacharya J, Konaré A, Martinez D, da Rocha R P, Sloan L C, Steiner A L (2007). The ICTP RegCM3 and RegCNET: regional climate modeling for the developing world. Bull Am Meteorol Soc, 88: 1395–1409

Steiner A L, Pal J S, Rauscher S A, Bell J L, Diffenbaugh N S, Boone A, Sloan L C, Giorgi F (2009). Land surface coupling in regional climate simulations of the West African monsoon. Clim Dyn, 33(6): 869–892

Subin Z M, Riley W J, Jin J (2011). Ecosystem Feedbacks to Climate Change in California: Development, Testing, and Analysis Using a Coupled Regional Atmosphere and Land Surface Model (WRF3–CLM3.5). Earth Interactions, vol. 15, Paper No. 15

Tang J P, Su B K, Zhao M (2003) Combinatorial optimization using MM5V3's various parameterizations in different physical processes: regional climate simulation in East Asia. Journal of Nanjing University (Natural Sciences), 39(16): 754–769

Tawfik A B, Steiner A L (2011). The role of soil ice in land–atmosphere coupling over the United States: a soil moistureprecipitation winter feedback mechanism. J Geophys Res, 116(D2): D02113

Wang C H, Sun C (2013). Design and preliminary test of the Regional Climate Model (WRFC) base on coupling WRFV3.2 and CLM4.0. Plateau Meteorology, 32(6): 1626–1637

Xu Y, Gao X J, Shen Y, Xu C H, Shi Y, Giorgi F (2009). A daily temperature dataset over China and its application in validating a

RCM simulation. Adv Atmos Sci, 26(4): 763–772

Yatagai A, Arakawa O, Kamiguchi K, Kawamoto H, Nodzu M I, Hamada A (2009). A 44-year daily gridded precipitation dataset for Asia based on a dense network of rain gauges. Science Online Letters on the Atmosphere, 5: 137–140

Yhang Y B, Hong S Y (2008). Improved physical processes in a regional climate model and their impact on the simulated summer monsoon circulations over East Asia. J Clim, 21(5): 963–979

Yu E T, Wang H J, Sun J Q (2010). A quick report on a dynamical downscaling simulation over China using the nested model. Atmos Oceanic Sci Lett, 3: 325–329

Zhang D F, Ouyang L C, Gao X J, Zhao Z C, Pal J S, Giorgi F (2007). Simulation of the atmospheric circulation over East Asia and climate in China by RegCM3. Journal of Tropical Meteorology, 23(5): 444–452

Zhao D (2013). Performance of regional integrated environment modeling system (RIEMS) in precipitation simulations over East Asia. Clim Dyn, 40(7−8): 1767–1787